Final Results of the Prospective Biomarker Trial PETra: [^{11}C]-MET-Accumulation in Postoperative PET/MRI Predicts Outcome after Radiochemotherapy in Glioblastoma

Annekatrin Seidlitz[1,2,3,4], Bettina Beuthien-Baumann[5,6], Steffen Löck[1,3,4], Christina Jentsch[1,2,3], Ivan Platzek[7], Klaus Zöphel[5], Annett Linge[1,2,3,4], Jörg Kotzerke[5], Jan Petr[8,11], Jörg van den Hoff[5,8], Jörg Steinbach[8,12], Dietmar Krex[9], Gabriele Schmitz-Schackert[9], Monique Falk[1,2,4], Michael Baumann[1,3,10,13], and Mechthild Krause[1,2,3,4,10]

ABSTRACT

Purpose: This prospective trial investigates the association of time to recurrence (TTR) in glioblastoma with [^{11}C]methionine (MET) tracer uptake before postoperative radiochemotherapy (RCT) aiming to guide radiotherapy boost regions.

Experimental Design: Between 2013 and 2016, 102 patients with glioblastoma were recruited. RCT was performed with concurrent and adjuvant temozolomide to a total dose of 60 Gy. Tumor residues in postresection PET and MRI were together defined as gross tumor volumes for radiotherapy treatment planning. [^{11}C]methionine (MET)-PET/MRI was performed before RCT and at each follow-up.

Results: The primary hypothesis of a longer TTR for patients without increased tracer accumulation in postoperative MET-PET was confirmed in 89 patients. With 18.9 months (95% confidence interval, 9.3–28.5 months), median TTR was significantly ($P < 0.001$) longer for patients without ($n = 29$, 32.6%) as compared with 6.3 months (3.6–8.9) for patients with MET accumulation ($n = 60$, 67.4%) in pre-RCT PET. Although MRI often did not detect all PET-positive regions, an unfavorable impact of residual tumor in postsurgical MRI ($n = 38$, 42.7%) on TTR was observed [4.6 (4.2–5.1) vs. 15.5 months (6.0–24.9), $P < 0.001$]. Significant multivariable predictors for TTR were MRI positivity, PET-positive volume, and O^6-methylguanine DNA methyltransferase (MGMT) hypermethylation.

Conclusions: Postsurgical amino acid PET has prognostic value for TTR after RCT in glioblastoma. Because of the added value of the metabolic beyond the pure structural information, it should complement MRI in radiotherapy planning if available with reasonable effort, at least in the context of maximal therapy. Furthermore, the spatial correlation of regions of recurrence with PET-positive volumes could provide a bioimaging basis for further trials, for example, testing local radiation dose escalation.

Introduction

Postoperative radiotherapy remains a mainstay clinical treatment for glioblastoma. The introduction of combined postoperative radiochemotherapy (RCT) more than 10 years ago (1) has for the first time led to a noticeable proportion of patients surviving 5 years after primary treatment. For prediction of the general prognosis of patients with glioblastoma, the recursive partitioning analysis classification in its original (2) or modified version (3) including patient's age, performance status, extent of surgery, tumor grading, and brain function, is widely used. Increasing evidence supports additional value of molecular markers and presence of isocitrate dehydrogenase (IDH) mutation and 1p/19q codeletion is now part of the World Health Organization (WHO) 2016 classification (4). However, none of these markers has become standard for treatment stratifications in clinical routine for glioblastoma (5). Several studies have tested escalated radiotherapy doses using recent techniques to improve outcome of radiotherapy in glioblastoma (6–14) and most of them showed higher local control rates and survival (7–11, 13, 15), sometimes at the price of higher toxicity. However, randomized data are missing, and some of

[1]Department of Radiation Oncology, Faculty of Medicine and University Hospital Carl Gustav Carus, Technische Universität Dresden, Dresden, Germany. [2]National Center for Tumor Diseases (NCT), Partner Site Dresden, Germany: German Cancer Research Center (DKFZ), Heidelberg, Germany; Faculty of Medicine and University Hospital Carl Gustav Carus, Technische Universität Dresden, Dresden, Germany, and Helmholtz Association/Helmholtz-Zentrum Dresden - Rossendorf (HZDR), Dresden, Germany. [3]OncoRay - National Center for Radiation Research in Oncology, Faculty of Medicine and University Hospital Carl Gustav Carus, Technische Universität Dresden, Helmholtz-Zentrum Dresden - Rossendorf, Dresden, Germany. [4]German Cancer Research Center (DKFZ), Heidelberg and German Cancer Consortium (DKTK) partner site, Dresden, Germany. [5]Department of Nuclear Medicine, Faculty of Medicine and University Hospital Carl Gustav Carus, Technische Universität Dresden, Dresden, Germany. [6]German Cancer Research Center (DKFZ), Department of Radiology, Heidelberg, Germany. [7]Institute of Radiology, Faculty of Medicine and University Hospital Carl Gustav Carus, Technische Universität Dresden, Dresden, Germany. [8]Helmholtz-Zentrum Dresden-Rossendorf, Institute of Radiopharmaceutical Cancer Research, Dresden, Germany. [9]Department of Neurosurgery, Faculty of Medicine and University Hospital Carl Gustav Carus, Technische Universität Dresden, Dresden, Germany. [10]Helmholtz-Zentrum Dresden-Rossendorf, Institute of Radiooncology, Dresden, Germany. [11]Department of Biomedical Engineering, Rochester Institute of Technology, Rochester, New York. [12]Department of Chemistry and Food Chemistry, TU Dresden, Dresden, Germany. [13]German Cancer Research Center (DKFZ), Heidelberg, Germany.

Note: Supplementary data for this article are available at Clinical Cancer Research Online (http://clincancerres.aacrjournals.org/).

Corresponding Author: Annekatrin Seidlitz, Medicine Faculty and University Hospital Carl Gustav Carus, Dresden 01309, Germany. Phone 49351-458-15693; E-mail: annekatrin.seidlitz@uniklinikum-dresden.de

Clin Cancer Res 2021;27:1351–60

doi: 10.1158/1078-0432.CCR-20-1775

Translational Relevance

Patients with glioblastoma still have a poor prognosis despite intense multimodal treatment. However, local treatments, such as high-precision radiotherapy have the potential to further improve local control. Therefore biomarkers are required not only to predict the risk but particularly the location of a recurrence. Amino acid PET/MRI is not a widely available method for diagnosis or radiotherapy treatment planning in glioblastoma but it is a widely promising approach to guide therapy intensification. While prospective data are scarce, retrospective evaluations suggest a superior diagnostic impact versus standard MRI and a colocalization of tracer uptake before standard radiochemotherapy (RCT) with later location of recurrence. This prospective trial confirms the impact of [^{11}C]-methionine-PET/MRI before postoperative radiochemotherapy of newly diagnosed glioblastoma in 89 patients. Tumor residues in PET were included in gross tumor volumes for radiotherapy treatment planning. Exploratory analysis showed a spatial correlation of the recurrence region with pre-radiochemotherapy PET tracer accumulation in the majority of patients, which could guide future dose-escalation trials.

these studies were retrospective and thus prone to selection bias. Still, precise definition of boost areas for dose escalation only in those patients with high risk of early locally confined recurrence might help to reduce severe late effects at improved local tumor control rates. For optimization of local treatments, such as high-precision radiotherapy, biomarkers are needed that do not only predict the risk but also the location of a recurrence. Although retrospective evaluations suggest a superior diagnostic value of pre-RCT amino acid PET with [11C]methionine (MET) versus MRI (16) and a colocalization of MET tracer uptake before standard RCT with later location of recurrence (17, 18), prospective data on this question are scarce. In a small prospective study on 34 patients, a spatial correlation of recurrences with the initially amino acid PET [O-(2–18F-fluoroethyl)-L-tyrosine (FET)]-positive areas was shown with no additional recurrences within initially MRI-positive areas (19).

The prospective study presented here aims to investigate the association of high MET tracer uptake before postoperative RCT and concurrent temozolomide with time to recurrence (TTR) in patients with glioblastoma. To gain information toward a potential individualized radiation dose-escalation strategy, secondary aims were definition of prognostic groups for TTR and to evaluate the spatial colocalization of recurrences with the initially MET-PET–positive areas.

Materials and Methods

Trial design

The PETra trial is a prospective one-arm, single-center, nonrandomized biomarker study. The study was conducted in accordance with the Declaration of Helsinki in the University Hospital/Faculty of Medicine Carl Gustav Carus of the Technische Universität Dresden (Dresden, Germany) in cooperation and with financial support of the German Cancer Consortium (DKTK)/German Cancer Research Center (DKFZ; Heidelberg, Germany) and the Helmholtz-Zentrum Dresden-Rossendorf (HZDR, Dresden, Germany). The protocol was reviewed and approved by the institutional review board (EK 41022013) and registered in a clinical trials database (clinicaltrials.gov; NCT01873469). All patients gave written informed consent.

Patients

Adult patients (age ≥ 18 years) with histologically confirmed newly diagnosed glioblastoma and clinical indication for standard RCT with temozolomide were consecutively recruited if they were in adequate general conditions (Karnofsky Performance Score ≥ 60, ECOG ≤ 2). RCT had to start within 7 weeks after surgery (macroscopic total tumor resection or biopsy allowed) and adequate contraception was required. Participation in other clinical trials was allowed, if not competing with the PETra trial. Exclusion criteria were previous radiotherapy of the brain, previous chemotherapy with temozolomide, other known malignant disease likely to affect survival prognosis and/or require interventions interfering with study treatment, pregnancy or lactation, claustrophobia and non–MRI-compatible material in the body (metal implants, pacemakers/defibrillators, insulin pumps, neurostimulators, cochlear implants).

Image acquisition and evaluation

MET-PET/MRI was performed before RCT and at each follow-up visit every 3 months until objective tumor recurrence. Details of image acquisition are given in Supplementary Data S1.

PET data of the timeframe of 20–40 minutes after injection were evaluated qualitatively and quantitatively. For visual comparison of different scans, the images were displayed using an SUV window of [0–4]. Qualitative evaluation comprised the evaluation of abnormal distribution of MET suspicious for tumor (i.e., focal uptake in areas without physiologically enhanced uptake and not compatible with postsurgical alteration). Tumor three-dimensional (3D) volumes of interest (VOI), encompassing the suspicious tumor area, were delineated by a nuclear medicine expert (B. Beuthien-Baumann), using the software package ROVER (ABX). The VOIs were defined manually by applying an adaptive threshold for each suspicious lesion, because using a fixed threshold led to erroneous delineations. Tumor VOIs were exported to the commercial treatment planning software RayStation (Version 6.0, RaySearch). MRI tumor volumes were recontoured (A. Seidlitz) for this evaluation in the treatment planning system as T1 contrast-enhancing regions in the first MRI 24–48 hours after surgery, considering nodular lesions as residual tumor and linear enhancement as posttherapeutic changes. Residual tumor status was dichotomized using primarily this early postsurgical MRI under auxiliary consideration of operative reports and the second baseline MRI obtained contemporaneously with PET. As the second MRI was a median 23 (minimum 9, maximum 45) days after surgical MRI, it is prone to unspecific changes. Therefore, residual tumor evaluation could change to MRI negative if the second MRI showed no residual tumor at all (false-positive postsurgical e.g., due to unspecific changes, blood, etc.). On the other hand, it could only change from negative to positive if there was conversion from missing residues in postsurgical scans to unambiguous macroscopic tumor in second MRI, that is, in case of distinct progression between these two pre-RCT scans. Difficult cases were independently reviewed by an experienced radiologist (I. Platzek).

For evaluation of spatial correlations with recurrences, treatment plans including the treatment volumes (information to follow) were rigidly coregistered with the follow-up images and with the contoured initial PET/MRI images (see above) in RayStation. Classification of the location of recurrences was initially done according to the proportion of the recurrence volume covered by the 95% isodose (V95) as follows: central recurrence if V95≥95%, in-field if 95%>V95≥80%, marginal if 80%>V95≥20% and distant if V95 <20% (20, 21). As this classification did not prove satisfactory to the assessment with respect to a future dose-escalation trial based on PET/MRI, it was adjusted for clinical

meaningful judgement and, all cases were reviewed together with the principal investigator (M. Krause) as follows: distant in case of no anatomic connection to the former primary tumor or resection cavity, local if within the region of former primary tumor or resection cavity and locoregional if local plus spread outside the V95. Anatomic shifts over time were carefully taken into consideration and visual classification corrected if necessary.

Treatment

Concurrent and adjuvant temozolomide was prescribed according to clinical standards (2). Certified commercial treatment planning systems were used for treatment planning. Images of the baseline diagnostic PET/MRI were coregistered to the planning CT. For target volume definition and follow-up imaging of this trial, the radiation oncologists were supported by the diagnostic imaging team, that is, specialists in radiology and in nuclear medicine. According to the clinical standard, the cavity plus contrast-enhancing lesion in MRI was delineated as gross tumor volume (GTV). Specific for the PETra study, the PET-positive volume was also included into the GTV. Tumor residues in PET or MRI were included in the GTVs. The GTV was expanded by a 20-mm or 5-mm isotropic margin to create the 50-Gy (RBE) or 60-Gy (RBE) clinical target volume (CTV) under consideration of anatomic borders, respectively. If nonenhancing lesions or edema in T2/FLAIR MRI were not included in this 20 mm margin, the CTV was enlarged to include these regions in line with clinical standards. Radiotherapy was applied with photons (6/15 MV linear accelerators, 3D conformal radiotherapy or intensity-modulated radiotherapy) or protons (100–230 MeV, double scattering technique, field shaping by range compensators and lateral apertures). As important processes, such as clinical target volume creation, were similar between the two treatment modalities and dose was normalized to the commonly accepted factor of 1.1 for the relative biological effectiveness, the effect of proton and photon therapy on tumor control are expected to be equal (22). Each treatment plan was approved by two radiation oncologists and two medical physicists. Constraint doses to organs at risk were used according to current clinical guidelines based on QUANTEC criteria (23–25).

Analysis of MGMT promoter methylation status

For the majority of patients ($n = 86$), the MGMT promoter methylation status was obtained in routine diagnostics using the Therascreen MGMT Pyro Kit (Qiagen GmbH). Samples with <8% methylation were considered nonmethylated (26, 27).

For three patients with missing MGMT status, MGMT methylation was determined using methylation-specific PCR. After the tumor content of the respective formalin-fixed paraffin-embedded (FFPE) tissues was estimated from hematoxylin and eosin–stained tissue sections by an experienced neuropathologist, tissues with <70% glioblastoma content were subjected to macrodissection. Extraction of genomic DNA was carried out from 5-μm FFPE sections using the QIAamp DNA FFPE Tissue Kit (Qiagen GmbH) following the instruction of the manufacturer. Bisulfite conversation and methylation-specific PCR has been carried out as described previously (28, 29). Quantifications of the optical signals of the methylated (M) and unmethylated (U) product were performed with ImageJ (Rasband, W.S., ImageJ, U.S. NIH, Bethesda, MD, https://imagej.nih.gov/ij/, 1997–2018), according to ref. 30. Samples with an M/U ratio = 0 were considered nonmethylated (28).

IDH1 IHC analyses

FFPE material from 85 patients was available for mutant IDH1 (R132H)-specific IHC analyses. Following deparaffinization and antigen retrieval in target retrieval solution (pH 6.1; Dako) for 28 minutes at 630 W, IHC staining was performed. Endogenous peroxidase activity was blocked (Peroxidase Block, Dako). Sections were then incubated with the monoclonal mouse anti-IDH1 (R132H) antibody (dilution 1:40; clone H09; dianova GmbH) in Dako REAL Antibody Diluent for 30 minutes. Negative control slides were incubated with corresponding IgG antibody control (Dako). The staining was visualized by 3,3′-Diaminobenzidine immunostaining (Dako REAL EnVision Detection System, Peroxidase/DAB, Rabbit/Mouse). Blinded samples were evaluated semiquantitatively. Tumors with strong cytoplasmic staining were considered positive for IDH1 (R132H) mutation (31).

Study endpoints, quality assurance, and statistical considerations

The primary hypothesis was that the TTR is shorter in patients with MET tracer uptake before RCT as compared with patients without such uptake. Secondary objectives were to study the association of overall survival (OS) with MET tracer uptake and the comparison of localization of MET uptake at baseline with subsequent sites of recurrence. The primary endpoint TTR and the secondary endpoint OS were calculated from the first day of radiotherapy to the date of event or censoring. Definite judgement for recurrences was postponed until confirmation in further follow-up scans in some inconclusive cases. Time of recurrence was then set to the first scan indicating progression.

Trial monitoring was performed 10 times during the trial duration, capturing adherence to protocol, correct documentation, and definition of recurrences for all patients at the first three monitorings and for at least 10% of all patients for all further monitorings. Before data evaluation, an additional final monitoring was performed to check correct documentation of the primary endpoints for all included patients.

For statistical planning and data analysis, a certified biostatistician (S. Löck) was involved. The necessary sample size for the primary endpoint of this trial was estimated for Cox proportional hazards regression. A sample size of 79 patients is needed if the HR of TTR between patient groups stratified by a median split of MET uptake is 2.0, the 90% confidence interval (CI) of this HR ($\alpha = 0.1$) does not contain the value 1.0 with a power of 90%, accrual rate is five patients per month and follow-up continues at least for 6 months after accrual of the last patient.

In secondary analyses, the impact of potential prognostic variables on the endpoints was evaluated using univariable Cox regression for continuous variables and the log-rank test for categorical variables. Significant parameters were included in a multivariable Cox regression model using forward variable selection with $P < 0.05$ for inclusion and $P > 0.1$ for exclusion. On the basis of the first and third quartiles of the corresponding linear predictors, patients were assigned to three risk groups. Differences between these risk groups in TTR and OS were evaluated by the log-rank test. Statistical analyses were performed using IBM SPSS Statistics 25 (IBM Corporation). Two-sided tests were performed and $P < 0.05$ were considered statistically significant without multiple testing correction.

Results

Patients

A trial overview is given in Supplementary Fig. S1. A checklist referring to reporting recommendations for tumor marker prognostic studies (REMARK criteria) is shown in Supplementary Table S4. From

August 2013 to September 2016, 102 patients were included. Thirteen patients (12.7%) dropped out of the study early. Reasons were missing slots for baseline PET/MRI ($n = 5$), repeated surgery without new baseline imaging ($n = 1$), changes in the therapeutic concept due to massive progression before RCT ($n = 5$), canceling of participation ($n = 1$), and the delayed start of RCT ($n = 1$). Eighty-nine patients remained for the final analysis of the primary endpoint TTR. Median follow-up was 17.2 months (range, 1.5–73.0 months) at the time of closure of the database for final data analysis (April 23, 2020). Baseline characteristics are shown in **Table 1**.

All patients received radiotherapy per protocol. Slight changes in overall treatment time or combined treatments are described in Supplementary Data S2.

Imaging

Baseline PET imaging showed elevated MET uptake in 60 of 89 patients (67.4%). In contrast, baseline MRI exhibited contrast enhancement indicating residual tumor in only 38 of 89 patients (42.7%). All patients except for one with residual tumors in MRI also showed MET accumulation in PET imaging, but only 37 of 60 (61.7%) of all patients with elevated MET uptake had a visible tumor residuum in MRI imaging (**Table 2**). MET-positive volumes ranged from 0.0 to 74 mL, the median was 1.3 mL. Median volume of residual tumors was 2.9 mL.

Primary endpoint TTR

At closure of the database, nine patients were still under follow-up without tumor recurrence (censored), whereas 77 patients developed recurrences. The remaining three patients were censored because of early death from pulmonary embolism (before first follow-up) and in two cases because a second-line chemotherapy was initiated by the treating oncologist without tumor recurrence (14 and 27 months follow-up).

Table 2. Comparison between accumulation of 11C-methionine and MRI contrast agent in pre-RCT PET + MRI.

		MET tracer accumulation		
		No	**Yes**	**Total**
Contrast enhancement in MRI	No	28	23	51
	Yes	1	37	38
	Total	29	60	89

Abbreviations: MET, methionine; MRI, magnetic resonance imaging.

The HR of MET accumulation for TTR determined in Cox regression was 2.46 (90% CI, 1.59–3.80; $P = 0.001$), confirming the primary hypothesis of this study. Median TTR in the whole patient group was 7.6 months (95% CI, 6.9–8.2 months; **Fig. 1A**). A significantly increased median TTR was observed for patients without pathologic MET accumulation [18.9 months (9.3–28.5)] compared with patients with pathologic MET accumulation [6.3 months (3.6–8.9)] in the pre-RCT PET (**Fig. 1C**). In addition, larger MET accumulation was associated with shorter TTR ($P < 0.001$). Patients without MET accumulation were mostly male ($P = 0.002$), showed more MGMT methylated tumors ($P = 0.043$), lower age ($P = 0.049$), and less residual tumor in MRI ($P < 0.001$; **Table 1**).

Although fewer patients showed residual tumor in MRI versus PET imaging (**Table 2**), residual tumor detected by postoperative MRI was also significantly associated with TTR [15.5 months (6.0–24.9) vs. 4.6 months (4.2–5.1), $P < 0.001$; **Fig. 1E**]. Although patients with

Table 1. Patient characteristics for all patients and for the subgroups of MET-negative and MET-positive patients.

	All patients (89)		MET-negative patients (29)		MET-positive patients (60)		
Characteristics	**Number**	**%**	**Number**	**%**	**Number**	**%**	***P***
Gender							
Male	53	59.6	24	82.8	29	48.3	
Female	36	40.4	5	17.2	31	51.7	**0.002**[a]
ECOG status							
0	47	52.8	20	69.0	27	45.0	
1	37	41.6	8	27.6	29	48.3	
2	5	5.6	1	3.4	4	6.7	0.11[a]
Resection							
Complete (in post-op. MRI)	51	57.3	28	96.6	23	38.3	
Partly (in post-op. MRI)	31	34.8	1	3.4	30	50.0	
Biopsy	7	7.9	0	0.0	7	11.7	<**0.001**[a]
MGMT							
Methylated	30	33.7	14	48.3	16	26.7	
Wild-type	59	66.3	15	51.7	44	73.3	**0.043**[a]
IDH							
Mutated	6	6.7	4	13.8	2	3.3	
Wild-type	79	88.8	25	86.2	54	90.0	
Unknown	4	4.5	0	0	4	6.7	0.081[a]
	Median (range)		**Median (range)**		**Median (range)**		***P***
Age (years)	58 (23–82)		53 (26–82)		60.5 (23–76)		**0.049**[b]
MET-positive volume (mL)	1.3 (0.0–74)		0 (0–0)		4.5 (0.1–74)		<**0.001**[b]
Postsurgical enhancing tumor volume in MRI (mL)	0.0 (0.0–41)		0 (0–8.9)		1.0 (0–41)		<**0.001**[b]

Note: The characteristics of the subgroups were compared by statistical tests.
Bold values indicate statistical significance $P < 0.05$
Abbreviations: ECOG, Eastern Co-operative Oncology Group; IDH, isocitrate dehydrogenase; MET, methionine; MGMT, O^6-methylguanine DNA methyltransferase.
[a]χ^2 test.
[b]Mann–Whitney *U* test.

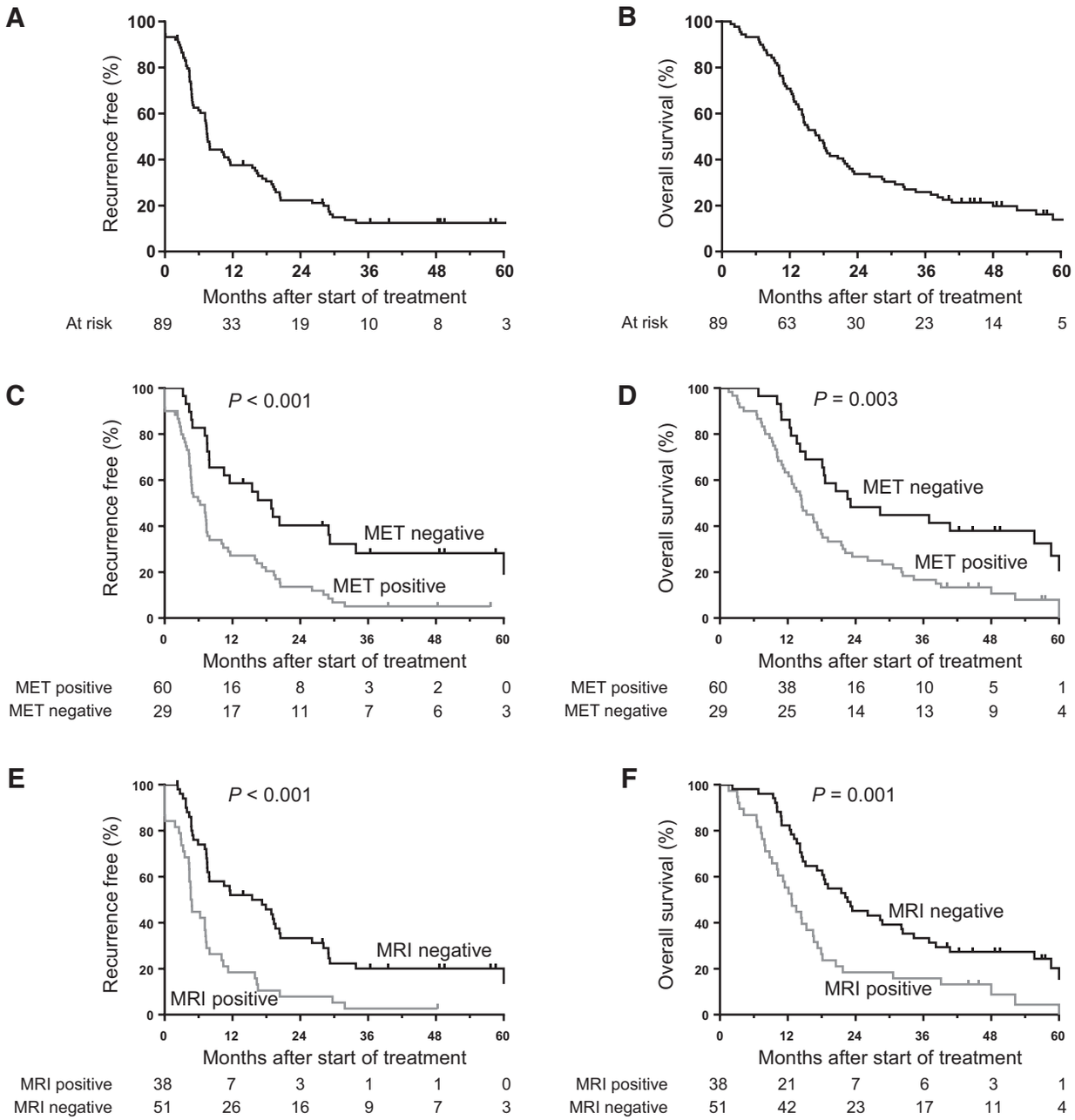

Figure 1.

Kaplan–Meier curves for freedom from tumor recurrence (**A**) and OS (**B**) for the whole patient cohort, for patient groups without versus with MET accumulation in the pre-RCT PET/MRI (**C** and **D**) and for patients with or without suspected tumor residuum in the 24-hour postoperative MRI (**E** and **F**).

residual tumor in MRI and PET showed the lowest TTR, patients without residual tumor in both analyses performed best and PET positivity but MRI negativity resulted in intermediate TTR (see Supplementary Fig. S3). No correlation with outcome was detected for performance status, presumably due to narrow inclusion criteria of the trial. Effect sizes of the considered patient characteristics for TTR were similar for patients with and without residual tumor in MRI (Supplementary Table S1).

Secondary endpoint OS

Thirteen patients were still alive, whereas 76 had died at the time of closure of the database. Median OS in the whole patient group was 17.2 months (95% CI, 13.6–20.7 months; **Fig. 1B**). OS differed between patients with MET-negative and MET-positive PET scans [23.1 months (9.4–36.8) vs. 14.5 months (12.2–16.8), $P = 0.003$] as well as between patients without and with contrast-enhancing tumor residuum in MRI [22.6 months (15.0–30.1) vs. 12.7 months

Table 3. Univariable and multivariable Cox regression of TTR and OS.

Variable	Univariable analyses		Multivariable analyses	
	HR (95% CI)	*P*	HR (95% CI)	*P*
Time to recurrence				
Age (years)	1.01 (1.00–1.03)	0.089		
Gender (female vs. male)	1.07 (0.67–1.69)	0.78		
ECOG status (0 vs. >0)	1.17 (0.75–1.83)	0.50		
MGMT (methylated vs. wild-type)	0.26 (0.16–0.44)	**<0.001**	0.20 (0.12–0.35)	**<0.001**
IDH (methylated vs. wild-type)	0.26 (0.08–0.82)	**0.022**		
MET accumulation (yes vs. no)	2.46 (1.47–4.13)	**0.001**		
MET-positive volume (mL)	1.04 (1.02–1.06)	**<0.001**	1.03 (1.01–1.06)	**0.004**
Postsurgical enhancing tumor volume in MRI (mL)	1.02 (0.99–1.04)	0.16		
Residuum in MRI (yes vs. no)	2.52 (1.59–4.00)	**<0.001**	2.74 (1.63–4.61)	**<0.001**
Overall survival				
Age (years)	1.03 (1.01–1.04)	**0.002**	1.04 (1.02–1.06)	**<0.001**
Gender (female vs. male)	0.95 (0.60–1.50)	0.81		
ECOG status (0 vs. >0)	1.27 (0.80–2.01)	0.30		
MGMT (methylated vs. wild-type)	0.26 (0.15–0.45)	**<0.001**	0.16 (0.08–0.29)	**<0.001**
IDH (methylated vs. wild-type)	0.32 (0.10–1.02)	0.054		
MET accumulation (yes vs. no)	2.15 (1.29–3.60)	**0.004**		
MET-positive volume (mL)	1.04 (1.01–1.06)	**0.002**	1.04 (1.02–1.07)	**0.002**
Postsurgical enhancing tumor volume in MRI (mL)	1.01 (0.98–1.04)	0.56		
Residuum in MRI (yes vs. no)	2.12 (1.34–3.35)	**0.001**	1.87 (1.11–3.14)	**0.018**

Abbreviations: ECOG, Performance Status according to Eastern Cooperative Oncology Group; MGMT, O^6-methylguanine DNA methyltransferase; IDH, isocitrate dehydrogenase; MET, [^{11}C]methionine; MRI, magnetic resonance imaging; HR, hazard ratio; 95% CI, 95 percent confidence interval.

(9.6–15.7), $P = 0.001$; **Fig. 1D** and **F**]. Larger MET accumulation was associated with shorter OS ($P = 0.002$). For progression-free survival (event: death or recurrence), similar results as for TTR were observed, shown in Supplementary Table S2. Although there is no clear standard treatment in case of recurrent glioblastoma, salvage therapy can impact OS. If performance status allowed further treatment, patients were discussed in interdisciplinary tumor boards. Recurrence surgery was performed in 47 patients; in 10 of them, there was more than one recurrence resection. In addition, 11 patients underwent another series of radiotherapy for recurrent glioblastoma. As salvage treatment is highly individual, it is not useful to account for this issue with statistical methods for this patient number.

Multivariable analysis

Parameters significantly related to TTR in univariable analysis were included in multivariable Cox regression with forward variable selection (**Table 3**). Although MGMT hypermethylation ($P < 0.001$), MET-positive volume ($P = 0.004$) and residual tumor in MRI ($P < 0.001$) remained significantly associated with TTR, PET positivity ($P = 0.33$) and IDH status ($P = 0.19$) were not selected. For OS, age was additionally selected ($P < 0.001$). Additional explorative statistical analyses, excluding the seven patients who underwent only biopsy, the four patients with clinical or histopathologic classification of secondary glioblastoma or the nine patients with mutated or unknown IDH status, yielded similar results in comparison with the whole cohort (not shown).

A risk score (rs) was defined on the basis of the linear predictor of the presented multivariable Cox model, $\text{rs} = -1.598 \times \text{MGMT} + 1.007 \times \text{MRI positivity} + 0.0328 \times \text{MET-positive volume (mL)}$. Using that risk score, three patient groups were exemplarily defined by the first and third quartiles, −0.635 and 0.971. The three risk groups differed significantly in TTR (all pairwise *P* values < 0.001; **Fig. 2**). Similarly, for OS the risk score was defined by $\text{rs} = -1.858 \times \text{MGMT} + 0.625 \times \text{MRI positivity} + 0.0413 \times \text{MET-positive volume (mL)} + 0.0401 \times \text{age (years)}$, and the quartiles were −0.972 and 0.929.

A freedom from recurrence rate of 59.3% and OS of 72.7% at 2 years, and a median TTR of 29.0 months (16.3–41.6) and OS of 48.0 months (15.7–80.4) was observed in the best prognosis group. In contrast, for the worst prognosis group, a freedom from recurrence rate of 0% and OS of 0% at 2 years, a median TTR of 4.3 months (2.8–5.8) and a median OS of 9.2 months (5.5–13.0) were observed.

To assess the impact of IDH mutation on the presented results, we performed an additional sensitivity analysis excluding the six patients with IDH-mutated tumors. Effect sizes for TTR and OS were similar in comparison to the analysis of the whole cohort (Supplementary Table S3; Supplementary Figs. S2 and S3). As expected, overall TTR and OS were slightly reduced because of the exclusion of the patients with IDH-mutated tumors with an inherent better prognosis.

Spatial correlation of recurrence regions with postoperative PET

At the time of closure of the database, 77 of 89 evaluable patients (86.5%) showed disease progression. In six of these patients (7.8%), no follow-up imaging was available due to early clinical progression during or shortly after RCT. All of these six patients had both MET-positive lesions and contrast-enhancing residual tumors in scans before therapy. Of the remaining 71 patients, 13 patients (18.3%) were imaged by MRI only at time of recurrence because of symptomatic progression and imaging performed outside the trial schedule, while 58 patients (81.7%) were imaged using PET/MRI at time of progression. These 71 patients (79.8% of the evaluated study population), were used for investigating the spatial correlation between the region of recurrence and baseline PET/MRI.

Relative to the high-dose irradiation volume, most patients developed local recurrences, but there were also some locoregional or distant failures or combinations (**Table 4**). Relative to the pre-RCT MET accumulation, of the 71 evaluable patients for this endpoint, the

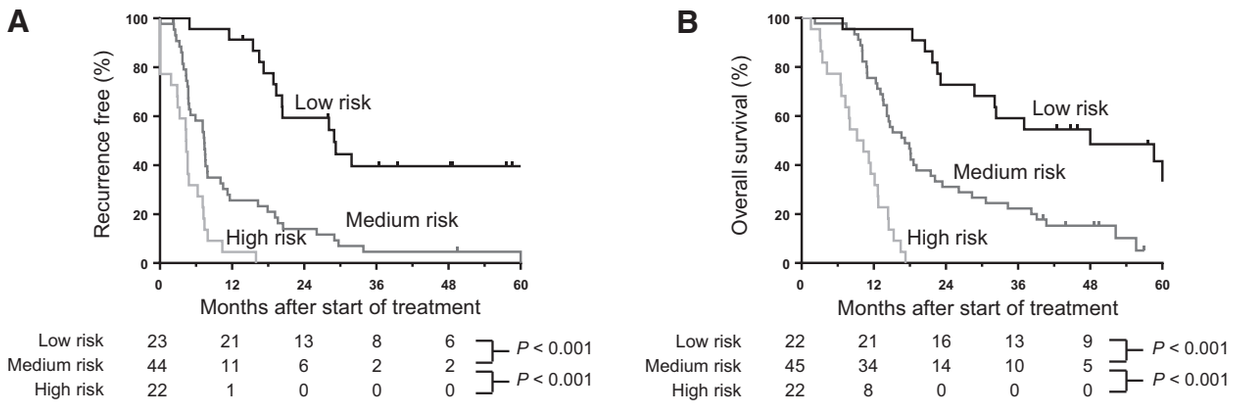

Figure 2.

Kaplan–Meier curves for freedom from tumor recurrence (**A**) and OS (**B**) for three risk groups combining MGMT hypermethylation, MET-positive volume, and residual tumor in MRI. The risk groups were defined by the first and third quartiles, −0.635 and 0.971 of the risk score (rs) based on the linear predictor of the presented multivariable Cox model, rs = −1.598 × MGMT + 1.007 × MRI positivity + 0.0328 × MET-positive volume (mL). Similarly, for OS the risk score was defined by rs = −1.858 × MGMT + 0.625 × MRI positivity + 0.0413 × MET-positive volume (mL) + 0.0401 × age (years), and the quartiles were −0.972 and 0.929.

recurrence occurred within the previously PET-positive area in 43 patients (60.6%). In 28 patients (39.4%), there was no pre-RCT tracer accumulation in the later recurrence region, either because these patients were initially PET-negative ($n = 21$) or because tracer accumulation before RCT and region of recurrence did not show spatial overlap ($n = 7$). Independent of the initial MET-positive region, in 57 patients (80.3%) tumor recurrence occurred at the resection margin. Of the 16 evaluable patients in the worst-prognosis group (**Fig. 2**), all recurrences occurred in the previously PET-positive area. For illustration, imaging before RCT and at time of recurrence 6 months thereafter of a 60-year-old patient after initial gross total resection is shown in **Fig. 3**.

Discussion

This prospective clinical trial confirmed our primary hypothesis that TTR is significantly shorter in patients with MET positivity in postresection PET imaging before RCT compared with MET-negative patients. More patients showed PET-positive areas after surgery as compared with MRI-positive areas (**Table 2**). Thus, PET negativity defined a patient group with longer TTR, while MRI positivity defined a group at particularly high risk of early recurrence (**Fig. 1**). Combining MRI positivity with MGMT status, age and MET-positive volume further improved its prognostic value. In line with retrospective data (32) and three prospective studies on 44 (33), 79 (34), and 16 patients (35), using FET-PET, our data underscore a high prognostic value of amino acid PET for patients with glioblastoma. FET and MET-PET have shown equivalence in a previous study (36).

In light of the importance of IDH status in the WHO 2016 classification (4), we performed a sensitivity analysis with exclusion of the six patients with IDH-mutated tumors showing similar results for TTR and OS. Patients with IDH mutation were not excluded for the main analyses; however, as IDH analysis was not clinical standard and also not part of glioblastoma classification at the time of patient diagnosis and treatment (2013–2016). Thus, it was also not part of the inclusion criteria. Nevertheless, results for the patients without IDH mutation are shown as Supplementary Materials, which allow for the comparison of the results with future publications according to the WHO 2016 classification (4).

PET-positive areas before RCT were not always located along the resection cavity, and in a sizable fraction of patients (38.3%; **Table 2**) they were not accompanied by contrast enhancement in MRI 24–72 hours after surgery. Thus, another important conclusion of this and also previous studies (14, 19, 37, 38) is, that amino acid PET has substantial value for precise target volume definition for radio(chemo) therapy.

To the best of our knowledge, we have for the first time prospectively shown an association of OS and freedom from recurrence with risk groups defined by MET-positive volume, MRI positivity, and MGMT hypermethylation status. Pending validation of this model is an important limitation, which should be addressed in future trials. Nevertheless, this prospectively obtained result is in line with

Table 4. Location of recurrences relative to the high-dose area of radiotherapy.

	Recurrence location		No. of patients	Percentage
Solely local	–	–	41	57.7
Local	+ Locoregional	–	13	18.3
Local	–	+Distant	7	9.9
Local	+ Locoregional	+Distant	3	4.2
–	Solely locoregional	–	0	0
–	Locoregional	+ Distant	1	1.4
–	–	Solely distant	6	8.5

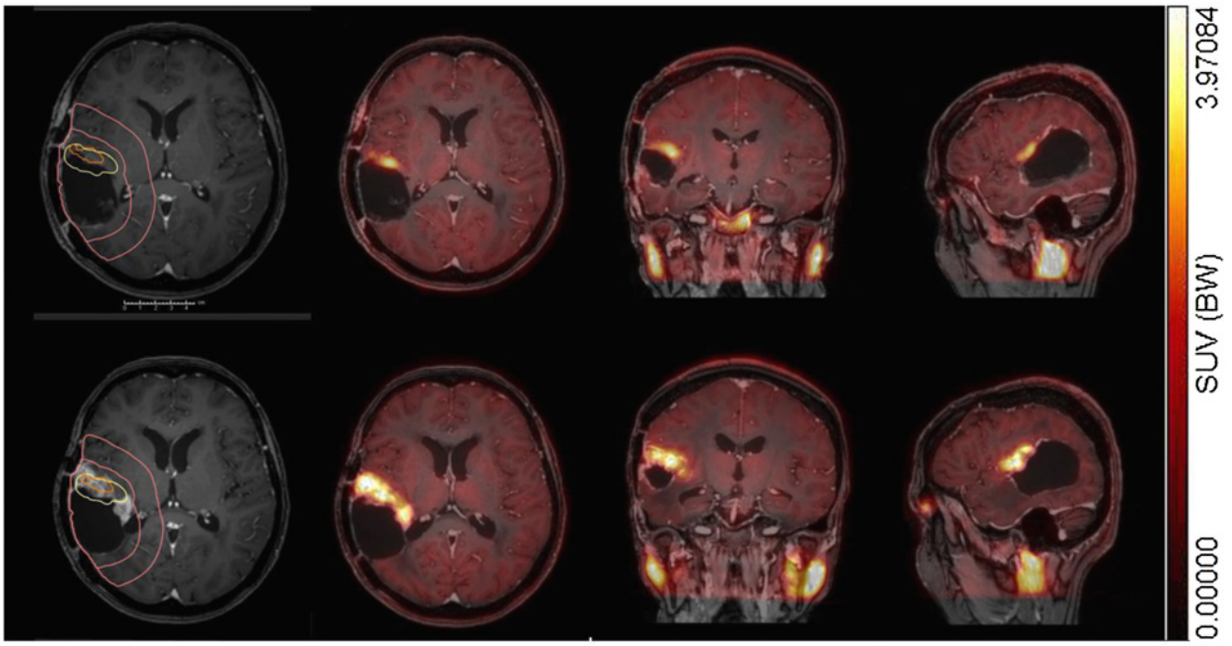

Figure 3.

Imaging before RCT (top row) and at time of recurrence 6 months thereafter (bottom row) of a 60-year-old patient after initial gross total resection is shown. MRI (T1 with contrast enhancement) is displayed in the left column beneath the fusion of this MRI with MET-PET in axial, coronal and sagittal direction. PET-positive volume according to the nuclear medicine expert (orange) in comparison with the radiooncologist (yellow) visualizes interobserver variability. The inner rose line surrounds the CTV prescribed with 60, the outer rose line the CTV prescribed with 50 Gy.

retrospective data, suggesting a prognosis score of MGMT status, biological tumor volume defined by amino acid PET, patient age, and performance status (32).

For an individualized radiation dose prescription strategy, besides the determination of the prognostic value of MET-PET and the definition of prognosis groups, the colocalization of recurrences with regard to pre-RCT MET accumulation is important to assess. In our study, for tumors that were PET positive before RCT, consecutive tumor recurrences occurred in the initially PET-positive region in 86.0% of cases (43/50). Only seven recurrences were found outside of the former PET-positive region. However, 21 additional patients developed recurrences without MET accumulation before RCT. Radiotherapy dose escalation to the PET-positive area (if present) would thus apply higher radiation dose in the region of highest risk of recurrence in 60.6% of the patients with recurrence, that is, would have a sensitivity of 60.6%. Of the nine patients who are still under follow-up without recurrence, three showed pre-RCT MET accumulation (33.3%). Those three patients would potentially have been overtreated with a local radiotherapy boost, that is, the specificity would be 66.7%. For another eight patients with initial PET-positive volume, a colocalization with recurrence was not evaluable due to early recurrence without follow-up PET (6) or due to death without recurrence (2). Another approach of radiotherapy dose escalation would be to boost the resection cavity instead of a PET-positive postsurgical residual tumor volume. Although this would increase the sensitivity to 80.3%, it would lead to a dose escalation in many patients of the low-risk group (PET-negative before RCT). Interestingly, in the worst-prognosis group according to our multivariable model, all recurrences occurred in initially PET-positive areas. This observation suggests that it may be promising to test a local boost concept in this very high-risk group.

A dose escalation applying 72 Gy to amino acid PET-positive areas (here FET) has been tested in a small single-arm prospective study on 13 patients with glioblastoma (39). While recurrent tumor volumes in FET-PET overlapped only to one-third with the boost target volume, potentially due to shrinking and shifting of the resection cavity, a simulated target volume of the initially FET-positive area plus a 7-mm margin covered a median of 100% (54–100) of the region of recurrences and was still smaller than a MRI-based definition of the boost region. This study supports our conclusion that initially PET-positive areas are at high risk for recurrences; however, it does not answer the question whether a local boost application to the PET-positive area would reduce the number of recurrences.

Conclusion

Postsurgical amino acid PET has prognostic value for TTR after RCT in glioblastoma. Because of the added value of the metabolic beyond the pure structural information, it should complement MRI in radiotherapy planning if available with reasonable effort, at least in the context of maximal therapy. Furthermore, the spatial correlation of regions of recurrence with PET-positive volumes could provide a bioimaging basis for further trials for example, testing local radiation dose escalation.

Authors' Disclosures

B. Beuthien-Baumann reports personal fees from Bracco and Roche Pharma AG outside the submitted work. M. Baumann attended an advisory board meeting of MERCK KGaA (Darmstadt) in the past 5 years, for which the University of Dresden received a travel grant. He further received funding for his research projects and for educational grants to the University of Dresden by Teutopharma GmbH (2011–2015), IBA (2016), Bayer AG (2016–2018), Merck KGaA (2014–open), and

Medipan GmbH (2014–2018). He is on the supervisory board of HI-STEM gGmbH (Heidelberg) for the German Cancer Research Center (DKFZ, Heidelberg) and also member of the supervisory body of the Charité University Hospital, Berlin. As former chair of OncoRay (Dresden) and present CEO and scientific chair of the German Cancer Research Center (DKFZ, Heidelberg), he has been or is still responsible for collaborations with a multitude of companies and institutions, worldwide. In this capacity, he discussed potential projects with and has signed/signs contracts for his institute(s) and for the staff for research funding and/or collaborations with industry and academia, worldwide, including but not limited to pharmaceutical corporations like Bayer, Boehringer Ingelheim, Bosch, Roche and other corporations like Siemens, IBA, Varian, Elekta, Bruker and others. In this role, he was/is further responsible for commercial technology transfer activities of his institute(s), including the DKFZ-PSMA617 related patent portfolio [WO2015055318 (A1), ANTIGEN (PSMA)] and similar IP portfolios. No disclosures were reported by the other authors.

Authors' Contributions

A. Seidlitz: Data curation, formal analysis, validation, investigation, visualization, methodology, writing-original draft, writing-review and editing. **B. Beuthien-Baumann:** Conceptualization, resources, data curation, formal analysis, supervision, investigation, visualization, writing-review and editing. **S. Löck:** Data curation, formal analysis, supervision, validation, visualization, writing-original draft, writing-review and editing. **C. Jentsch:** Conceptualization. **I. Platzek:** Formal analysis, validation, writing-review and editing. **K. Zöphel:** Conceptualization, resources. **A. Linge:** Validation, investigation, methodology, writing-review and editing. **J. Kotzerke:** Conceptualization, resources. **J. Petr:** Resources, data curation, methodology, writing-review and editing. **J. van den Hoff:** Conceptualization, resources, funding acquisition. **J. Steinbach:** Conceptualization, resources, funding acquisition. **D. Krex:** Conceptualization, resources, supervision, writing-review and editing. **G. Schmitz-Schackert:** Conceptualization, resources. **M. Falk:** Conceptualization, project administration. **M. Baumann:** Conceptualization, resources, supervision, funding acquisition, project administration, writing-review and editing. **M. Krause:** Conceptualization, resources, supervision, funding acquisition, writing-original draft, project administration, writing-review and editing.

Acknowledgments

The support by the clinical trials center, especially the study nurses Annett and Susanne Klöber, Luisa Schünzel, Aline Lähner, and Nicole Jähnel; as well as the data officers Ulrike Junker, Romy Schöne, and Evelin Klatt is gratefully acknowledged. We thank Rebecca Bütof for support with clinical queries.

We also thank the medical physicists Kristin Stützer, Annika Jacobi, and Patrick Wohlfahrt as well as the data scientist and manager of the RadPlanBio-database Tomas Skripcak for the very helpful support.

Finally, the authors gratefully acknowledge the excellent technical assistance by Liane Stolz-Kieslich, Sigrid Ermscher, Daniela Friede and Andrea Petzold. The authors also wish to thank the Tumour and Normal Tissue Bank of the University Cancer Center of the University Hospital Dresden (TNTB, Daniela Aust) and the neuropathologist Matthias Meinhardt.

This investigator initiated trial was conducted in cooperation and with financial support of the German Cancer Consortium (DKTK)/German Cancer Research Center (DKFZ) Heidelberg and the Helmholtz-Zentrum Dresden-Rossendorf (HZDR).

The costs of publication of this article were defrayed in part by the payment of page charges. This article must therefore be hereby marked *advertisement* in accordance with 18 U.S.C. Section 1734 solely to indicate this fact.

Received May 11, 2020; revised July 24, 2020; accepted December 22, 2020; published first December 29, 2020.

References

1. Stupp R, Mason WP, van den Bent MJ, Weller M, Fisher B, Taphoorn MJB, et al. Radiotherapy plus concomitant and adjuvant temozolomide for glioblastoma. N Engl J Med 2005;352:987–96.
2. Scott CB, Scarantino C, Urtasun R, Movsas B, Jones CU, Simpson JR, et al. Validation and predictive power of Radiation Therapy Oncology Group (RTOG) recursive partitioning analysis classes for malignant glioma patients: a report using RTOG 90–06. Int J Radiat Oncol Biol Phys 1998;40:51–5.
3. Mirimanoff R-O, Gorlia T, Mason W, Van den Bent MJ, Kortmann R-D, Fisher B, et al. Radiotherapy and temozolomide for newly diagnosed glioblastoma: recursive partitioning analysis of the EORTC 26981/22981-NCIC CE3 phase III randomized trial. J Clin Oncol 2006;24:2563–9.
4. Wesseling P, Capper D. WHO classification of gliomas. Neuropathol Appl Neurobiol 2017;44:139–50.
5. Weller M, van den Bent M, Tonn JC, Stupp R, Preusser M, Cohen-Jonathan-Moyal E, et al. European Association for Neuro.Oncology (EANO) guideline on the diagnosis and treatment of adult astrocytic and oligodendroglial gliomas. Lancet Oncol 2017;18:e315–29.
6. Weller M, Wick W, Hegi ME, Stupp R, Tabatabai G. Should biomarkers be used to design personalized medicine for the treatment of glioblastoma? Future Oncol 2010;6:1407–14.
7. Mizumoto M, Yamamoto T, Ishikawa E, Matsuda M, Takano S, Ishikawa H, et al. Proton beam therapy with concurrent chemotherapy for glioblastoma multiforme: comparison of nimustine hydrochloride and temozolomide. J Neurooncol 2016;130:165–170.
8. Tanaka M, Ino Y, Nakagawa K, Tago M, Todo T. High-dose conformal radiotherapy for supratentorial malignant glioma: a historical comparison. Lancet Oncol 2005;6:953–60.
9. Fitzek MM, Thornton AF, Rabinov JD, Lev MH, Pardo FS, Munzenrider JE, et al. Accelerated fractionated proton/photon irradiation to 90 cobalt gray equivalent for glioblastoma multiforme: results of a phase II prospective trial. J Neurosurg 1999;91:251–60.
10. Iuchi T, Hatano K, Kodama T, Sakaida T, Yokoi S, Kawasaki K, et al. Phase 2 trial of hypofractionated high-dose intensity modulated radiation therapy with concurrent and adjuvant temozolomide for newly diagnosed glioblastoma. Int J Radiat Oncol Biol Phys 2014;88:793–800.
11. Zschaeck S, Wust P, Graf R, Misch M, Onken J, Ghadjar P, et al. Locally dose-escalated radiotherapy may improve intracranial local control and overall survival among patients with glioblastoma. Radiat Oncol 2018;13:251.
12. Souhami L, Seiferheld W, Brachman D, Podgorsak EB, Werner-Wasik M, Lustig R, et al. Randomized comparison of stereotactic radiosurgery followed by conventional radiotherapy with carmustine to conventional radiotherapy with carmustine for patients with glioblastoma multiforme: report of Radiation Therapy Oncology Group 93–05 protocol. Int J Radiat Oncol Biol Phys 2004;60:853–60.
13. Tsien C, Moughan J, Michalski JM, Gilbert MR, Purdy J, Simpson J, et al. Phase I three-dimensional conformal radiation dose escalation study in newly diagnosed glioblastoma: Radiation Therapy Oncology Group Trial 98–03. Int J Radiat Oncol Biol Phys 2009;73:699–708.
14. Tsien CI, Brown D, Normolle D, Schipper M, Piert M, Junck L, et al. Concurrent temozolomide and dose-escalated intensity-modulated radiation therapy in newly diagnosed glioblastoma. Clin Cancer Res 2012;18:273–9.
15. Kim MM, Speers C, Li P, Schipper M, Junck L, Leung D, et al. Dose-intensified chemoradiation is associated with altered patterns of failure and favorable survival in patients with newly diagnosed glioblastoma. J Neurooncol 2019;143:313–9.
16. Wang Y, Rapalino O, Heidari P, Loeffler J, Shih HA, Oh K, et al. C11 methionine PET (MET-PET) imaging of glioblastoma for detecting postoperative residual disease and response to chemoradiation therapy. Int J Radiat Oncol Biol Phys 2018;102:1024–8.
17. Lee IH, Piert M, Gomez-Hassan D, Junck L, Rogers L, Hayman J, et al. Association of 11C-methionine PET uptake with site of failure after concurrent temozolomide and radiation for primary glioblastoma multiforme. Int J Radiat Oncol Biol Phys 2009;73:479–85.
18. Navarria P, Reggiori G, Pessina F, Ascolese AM, Tomatis S, Mancosu P, et al. Investigation on the role of integrated PET/MRI for target volume definition and radiotherapy planning in patients with high grade glioma. Radiother Oncol 2014;112:425–9.
19. Harat M, Malkowski B, Makarewicz R. Pre-irradiation tumour volumes defined by MRI and dual time-point FET-PET for the prediction of glioblastoma multiforme recurrence: a prospective study. Radiother Oncol 2016;120:241–7.
20. Weber DC, Casanova N, Zilli T, Buchegger F, Rouzaud M, Nouet P, et al. Recurrence pattern after [(18)F]fluoroethyltyrosine-positron emission

tomography-guided radiotherapy for high-grade glioma: a prospective study. Radiother Oncol 2009;93:586–92.
21. Chan JL, Lee SW, Fraass BA, Normolle DP, Greenberg HS, Junck LR, et al. Survival and failure patterns of high-grade gliomas after three-dimensional conformal radiotherapy. J Clin Oncol 2002;20:1635–42.
22. Mohan R, Grosshans D. Proton therapy - present and future. Adv Drug Deliv Rev 2017;109:26–44.
23. Lawrence YR, Li XA, el Naqa I, Hahn CA, Marks LB, Merchant TE, et al. Radiation dose-volume effects in the brain. Int J Radiat Oncol Biol Phys 2010;76: S20–7.
24. Mayo C, Martel MK, Marks LB, Flickinger J, Nam J, Kirkpatrick J. Radiation dose-volume effects of optic nerves and chiasm. Int J Radiat Oncol Biol Phys 2010;76:S28–35.
25. Mayo C, Yorke E, Merchant TE. Radiation associated brainstem injury. Int J Radiat Oncol Biol Phys 2010;76:S36–41.
26. Felsberg J, Thon N, Eigenbrod S, Hentschel B, Sabel MC, Westphal M, et al. Promoter methylation and expression of MGMT and the DNA mismatch repair genes MLH1, MSH2, MSH6 and PMS2 in paired primary and recurrent glioblastomas. Int J Cancer 2011;129:659–70.
27. Gurrieri L, De Carlo E, Gerratana L, De Maglio G, Macerelli M, Pisa FE, et al. MGMT pyrosequencing-based cut-off methylation level and clinical outcome in patients with glioblastoma multiforme. Future Oncol 2018;14:699–707.
28. Christians A, Hartmann C, Benner A, Meyer J, von Deimling A, Weller M, et al. Prognostic value of three different methods of MGMT promoter methylation analysis in a prospective trial on newly diagnosed glioblastoma. PLoS One 2012; 7:e33449.
29. Meneceur S, Linge A, Meinhardt M, Hering S, Löck S, Bütof R, et al. Establishment and characterisation of heterotopic patient-derived xenografts for glioblastoma. Cancers 2020;12:871.
30. Esteller M, Garcia-Foncillas J, Andion E, Goodman SN, Hidalgo OF, Vanaclocha V, et al. Inactivation of the DNA-repair gene MGMT and the clinical response of gliomas to alkylating agents. N Engl J Med 2000;343:1350–4.
31. Capper D, Weissert S, Balss J, Habel A, Meyer J, Jäger D, et al. Characterization of R132H mutation-specific IDH1 antibody binding in brain tumors. Brain Pathol 2010;20:245–54.
32. Poulsen SH, Urup T, Grunnet K, Christensen IbJ, Larsen VA, Jensen ML, et al. The prognostic value of FET PET at radiotherapy planning in newly diagnosed glioblastoma. Eur J Nucl Med Mol Imaging 2017;44:373–81.
33. Piroth MD, Holy R, Pinkawa M, Stoffels G, Kaiser HJ, Galldiks N, et al. Prognostic impact of postoperative, pre-irradiation (18)F-fluoroethyl-l-tyrosine uptake in glioblastoma patients treated with radiochemotherapy. Radiother Oncol 2011;99:218–24.
34. Suchorska B, Jansen NL, Linn J, Kretzschmar H, Janssen H, Eigenbrod S, et al. Biological tumor volume in 18FET-PET before radiochemotherapy correlates with survival in GBM. Neurology 2015;84:710–9.
35. Lundemann M, Munck Af Rosenschold P, Muhic A, Larsen VA, Poulsen HS, Engelholm S-A, et al. Feasibility of multi-parametric PET and MRI for prediction of tumour recurrence in patients with glioblastoma. Eur J Nucl Med Mol Imaging 2019;46:603–13.
36. Grosu A-L, Astner ST, Riedel E, Nieder C, Wiedenmann N, Heinemann F, et al. An interindividual comparison of O-(2-[18F]fluoroethyl)-L-tyrosine (FET)- and L-[methyl-11C]methionine (MET)-PET in patients with brain gliomas and metastases. Int J Radiat Oncol Biol Phys 2011;81:1049–58.
37. Lohmann P, Stavrinou P, Lipke K, Bauer EK, Ceccon G, Werner J-M, et al. FET PET reveals considerable spatial differences in tumour burden compared to conventional MRI in newly diagnosed glioblastoma. Eur J Nucl Med Mol Imaging 2019;46:591–602.
38. Hayes AR, Jayamanne D, Hsiao E, Schembri GP, Bailey DL, Roach PJ, et al. Utilizing 18F-fluoroethyltyrosine (FET) positron emission tomography (PET) to define suspected nonenhancing tumor for radiation therapy planning of glioblastoma. Pract Radiat Oncol 2018;8:230–8.
39. Piroth MD, Galldiks N, Pinkawa M, Holy R, Stoffels G, Ermert J, et al. Relapse patterns after radiochemotherapy of glioblastoma with FET PET-guided boost irradiation and simulation to optimize radiation target volume. Radiat Oncol 2016;11:87.